Learning Audio-Visual Dynamics Using Scene Graphs

Anonymous Author(s)
Affiliation
Address
email

Abstract

There exists an unequivocal distinction between the sound produced by a static agent and that produced by a moving one, especially when the agent moves towards or away from the microphone. In this paper, we propose to use this connection between audio and visual dynamics for solving two challenging tasks simultaneously, namely: (i) separating audio sources from a mixture using visual cues, and (ii) predicting the 3D visual motion of a sounding source only using its separated audio. Towards this end, we present Audio Separator and Motion Predictor (ASMP) – a deep learning framework that leverages the 3D structure of the scene and the motion of sound sources for better audio source separation. At the heart of ASMP is a pseudo-3D scene graph capturing various objects in the video and their 3D spatial proximities. This graph is constructed by registering together 2.5D monocular depth predictions from the 2D video frames and associating the 2.5D scene regions with the outputs of an object detector applied on those frames. The audio separation task is then modeled, as a joint problem of: (i) recursively segmenting the pseudo-3D scene graph into several sub-graphs, with each associated with a constituent sound of the mixed input audio, and (ii) predicting the 3D motions of the corresponding sound sources from the separated audio. To empirically evaluate ASMP, we present experiments on two challenging audio-visual datasets, viz. Audio Separation in the Wild (ASIW) and Audio Visual Event (AVE). Our results demonstrate that ASMP achieves a clear improvement in source separation quality, outperforming prior works on both datasets, while estimating the direction of motion of the sound sources better than other methods.

1 Introduction

Events around us are often audio-visual in nature and our senses have evolved to leverage this multimodal synergy to better reason about the world. For example, the sight of a baby smiling allows us to associate *a chuckling sound* with the kid, even when a myriad of other acoustic sources, such as television, car honks, etc. are present. In this paper, we propose to leverage this synergy between sight and sound for solving two challenging tasks simultaneously, viz.: (i) separating audio sources from a mixture using visual cues, and (ii) the novel task of predicting the 3D visual motion of the sounding source using only its separated audio.

Typical approaches to visually guided audio source separation use weakly- or self- supervised models trained to separate a mixture of acoustic sources into its constituents by conditioning on appropriate visual regions [52, 51, 11, 42, 7]. Such approaches impose constraints on the space of the separated audio (e.g., cyclic consistency, object identifiability, etc.) to derive gradients for training the underlying neural models. Some of them additionally seek to ground the separated audio with the appearance of the sounding object [42, 11, 7]. Chatterjee *et al.* [7], construct a 2D scene graph on the video frames to capture the visual context of the audio source for better separation; their key intuition being that certain sounding objects (e.g., a guitar) cannot produce the sound by itself, but

Submitted to 36th Conference on Neural Information Processing Systems (NeurIPS 2022). Do not distribute.

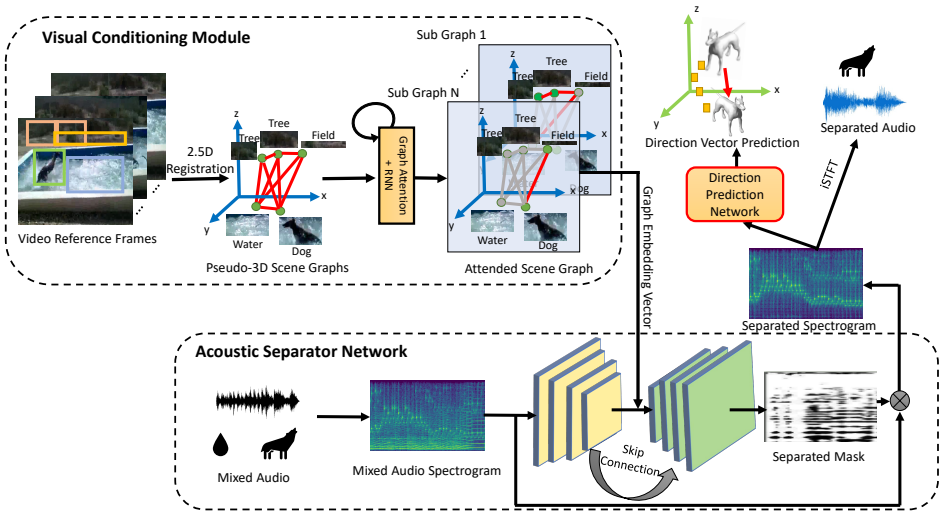

Figure 1: A detailed illustration of our proposed ASMP model.

must have a suitable spatial context around them (e.g., a person). However, all the above approaches ignore one key aspect of the physical world – that it is three dimensional and this 3D structure influences the sound being heard. For example, if *a person playing a guitar* is spatially distant from the microphone, then the audio mixture to be separated is unlikely to have the sound of that guitar. Further, the 3D scene structure also allows for incorporating the motion of sounding objects. Imagine *the whistling of a train moving towards you*. There is an inevitable relationship between the evolution of the sound of the train being heard and its 3D motion, which can help distinctly separate its sound from other whistling trains or background clamour and vice-versa. Thus, if the audio of this train is well-separated, then the separated audio must also be able to predict the direction of the train's motion. Leveraging these insights, we present Audio Separator and Motion Predictor (ASMP) – an innovative graph neural network for video-conditioned audio source separation from an acoustic mixture that can also predict the direction of motion of the sound source.

Our ASMP framework begins by computing a dense 2.5D representation of the frames of a video where 2.5D refers to the 2D visual context of the frames enriched with the pseudo-depth for that frame produced using a 2D-to-3D monocular depth prediction method [35]. Next, we succinctly capture the semantic context of this 2.5D visual scene by means of a novel 2.5D scene graph representation. The nodes of this scene graph capture the various objects in the scene (projected onto the pseudo-3D scene via the depth map), while the graph edges characterize the approximate 3D spatial distances between the objects. To achieve audio source separation, we propose a recurrent graph neural network that is trained to segment this 2.5D scene graph into sub-graph embeddings; each of which is trained to be associated with a potentially unique *sounding object or interaction* and is used to induce separation of that sound source from the audio mixture. To enforce this uniqueness, we impose orthogonality constraints between the generated graph embeddings. Moreover, ASMP is also capable of predicting the 3D direction of motion of a sounding object from its corresponding separated audio (see Figure 1).

The efficacy of ASMP on the dual tasks of sound source separation and motion direction prediction is evaluated by comparing its performances against related prior works on two recently introduced, challenging datasets, namely (i) Audio Separation in the Wild (ASIW) [7] and (ii) Audio Visual Event (AVE) [43]. Both of these datasets feature videos of sounding objects and interactions *in the wild*. ASMP is shown to outperform competing counterparts on both tasks, underscoring the importance of incorporating 3D spatial structure for both tasks. The success at the task of predicting the direction of motion from the separated audio, further suggests ASMP's applicability in a variety of other audio-visual problems, including occlusion reasoning, and video generation from audio [6].

Below we summarize the key contributions of the paper:

- We introduce a novel *3D geometry-aware scene graph representation* [18] for visually-guided audio source separation, called ASMP.
- We introduce a novel task of *predicting 3D motion direction* of a sound source in the scene from the the temporal evolution of the sound it makes and use it to improve audio separation.
- ASMP demonstrates *state-of-the-art* audio source separation and motion prediction performances on two challenging datasets for this task, viz. ASIW and AVE.

2 Related Works

Below we briefly review some of the important prior works that we build upon or techniques that are closely related to our approach.

Visually-guided Audio Source Separation is the task of separating a mixture of audio signals into its constituent sources by discovering the association between the separated sound sources and their visual appearances in the physical world. Typical methods for solving this task find a wide range of real-world applications, such as separating sounds of musical instruments [11, 9, 51, 52], separating speech signals [1, 8, 30], and separating on-screen sounds from off-screen ones for generic objects [32, 44]. A learning pipeline often used to train such methods conditions a sound-separation network (such as a U-net [37]) with an appropriate visual object representation, to induce a source separation on a mixed audio input, obtained by mixing the audio streams of two different videos. In recent years, research in this area has moved from using global visual features of motion and appearance [51] towards extracting very fine-grained visual conditioning information to induce more effective and precise separations [11, 42]. Additional refinement steps have also been explored [7] to ward off potential false separation triggers. However, none of these approaches factor the 3D geometry of the scene captured by the video into the visual representation – an important gap that we attempt to fill using ASMP. Moreover, by predicting the motion vector of the sound source from the audio, ASMP combines the separated audio and the corresponding visual information more closely.

Localizing Sound in Video Frames has been attempted in several recent methods by learning to ground the sound source in the visual space, e.g., identifying the pixels of the sound source [3, 38, 19, 15, 42]. While, these approaches strive to learn the association between the visual appearance and acoustic signatures of sound sources, they do not apply such methods to audio source separation – a task that is the focus of this work.

Sound Synthesis from Videos constitutes another category of important techniques in the audio-visual realm [33, 53] that has become popular lately. Towards this end, several approaches have recently been proposed for the task of generating both monaural and binaural audio starting from videos [10, 31, 49, 25]. However, differently, we seek to solve the task of sound source separation and motion prediction in the visual space.

Application of Scene Graphs to Videos has resulted in massive strides in video understanding tasks. Scene graphs, while traditionally used for capturing the static content of images [18, 26] have lately been used for several video understanding tasks. For instance, Ji *et al.* [17] applied them for action recognition, Geng *et al.* [12] for visual dialog, and Chatterjee *et al.* [7] for visually guided sound-source separation. However, their scene graphs are usually 2D, while we attempt to explicitly incorporate the 3D scene geometry into the scene graphs.

Audio Separation Using Direction of Arrival has been an important topic of recent interest in the audio research community [48, 40], where the direction of arrival of sound to a microphone array is explicitly used for improved sound source separation. While, our approach is inspired by their key findings, we attempt to explore this in the audio-visual domain.

3 Proposed Method

3.1 Task Setup and Method Overview

Let V denote an unlabeled video, and $m(t) = \sum_{i=1}^{N} \mathbf{a}_i(t)$ be its accompanying discrete-time audio arising from a linear mixture of N acoustic sources $\mathbf{a}_i(t)$. The main goal of *visually-guided audio source separation* is to use cues derived from V to induce a separation of $m(t)$ into its constituent acoustic sources $\mathbf{a}_i(t)$, for $i \in \{1, 2, \ldots, N\}$. For efficient reasoning, we represent the video V semantically as a scene graph $\mathcal{G} = (\mathcal{V}, \mathcal{E})$ with nodes $\mathcal{V} = \{n_1, n_2, \ldots, n_K\}$ denoting the objects in V and $\mathcal{E}$ capturing the set of edges e_{ij} characterizing the spatial proximity of a pair of nodes (n_i, n_j). The key idea in our proposed Audio Separator and Motion Predictor (ASMP) framework is to map each of the acoustic sources $\mathbf{a}_i(t)$ to a sub-graph of $\mathcal{G}$. We realize this mapping by auto-regressively partitioning the graph $\mathcal{G}$ into mutually-orthogonal neural embeddings and using these embeddings to condition an *Acoustic Separator* sub-network tasked with extracting a sound source $\mathbf{a}_i(t)$ from the mixture $m(t)$. A key ingredient in our model is equipping the audio separator to also predict the direction of motion of the sounding object. We incorporate this ability by including a direction prediction training loss. Figure 1 provides an overview of our model, and the details follow.

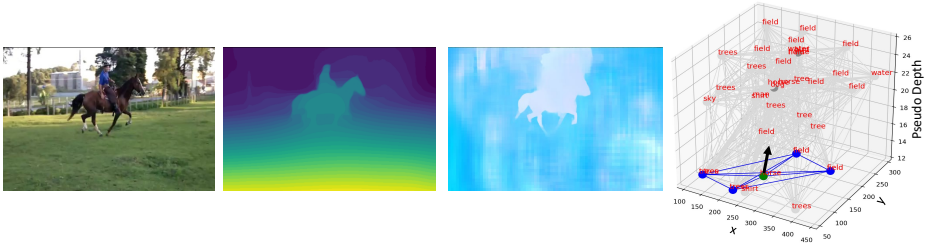

Reference Frame Pseudo-Depth Image Optical Flow Pseudo-3D Scene Graph

Figure 2: A step-wise illustration of the pseudo-3D scene graph construction process on an example frame from an ASIW video. We show the original frame, its predicted monocular 3D depth map, its optical flow estimate with an adjacent frame, and a pseudo-3D scene graph for the video. The highlighted part of the graph (blue edges) is the sub-graph associated with the sound of the horse's motion, while the black-arrow denotes the direction of the motion of the horse in 3D space.

3.2 Estimating Ground Truth Sound Source Motion

One novel aspect of ASMP is that it can predict the motion direction of a source from its sound. However, the ground truth for this task is not directly available from the 2D frames of a given video. In the following, we detail the pre-processing steps for estimating this ground truth, while an overview is shown in Figure 2. We denote a motion displacement vector, as $\mathbf{d}_i$ for the source $\mathbf{a}_i(t)$, which will be subsequently used as an auxiliary cue to train the audio source separator.

Computing Pseudo-Depth Maps: Constructing a 3D scene from 2D images is a classic problem explored in computer vision for which a variety of solutions exist[2, 13]. However, many of these methods make strong assumptions, such as: (i) the scene being static, (ii) existence of sufficient overlap between the frames, or (iii) knowledge of the intrinsic parameters of the camera, none of which may be feasible for the type of videos that are typically used in our task. To this end, we propose to build upon the recent progress made in monocular 3D reconstruction realm towards mapping each video frame F_f of V into a 2.5D pseudo-depth image [50]. In particular, we use the MiDAS algorithm [35] because of its ease-of-use and accuracy of depth predictions.

Rectifying Frames for Camera Motion. Since we do not assume that the frames in V have been captured by a static camera, we next align them to a common 3D reference frame F_r. To this end, we apply the classic *Lucak-Kanade* tracker [28] across the frames. As there may be objects moving out of the scene or shot-switches in the video, we found that tracking the *static objects* in the video typically does not sustain its full length. Thus, we group the frames into fixed-size windows, each with a maximum of ℓ continuous frames. A video can therefore, be considered as a collection of W windows, with each window producing its own motion displacement vector. This consequently also implies that our frames are aligned (rectified) within their respective windows. Concretely, let $\mathbf{x}$ denote a tracked point, in pseudo 3D, within a window. Suppose $\mathbf{x}_f \in \mathbb{R}^3$ and $\mathbf{x}_r \in \mathbb{R}^3$ be the 3D coordinate corresponding to $\mathbf{x}$ in F_f and that in the reference frame F_r, respectively. Then, using the full set of such tracked points in this window, we rectify F_f to F_r by estimating a 3D transformation matrix using the iterative closest point (ICP) algorithm [5]. Once the target frame F_f has been rectified, we also rectify its corresponding pseudo-depth map using the same transformation matrix.

Visual Detection of Sound Sources. To construct our scene graph, we first use a Faster-RCNN (FRCNN) [36] model for detecting a set of M objects and their 2D spatial bounding boxes in the reference frame F_r of a window. The detection model is trained (on the Visual Genome dataset [23]) to recognize and localize 1600 commonplace object classes. However, some of the data that we use in our experimental study consists of sound producing objects that are not in the Visual Genome classes list. To accommodate such classes (e.g., musical instruments), we use a separate FRCNN model pre-trained on images annotated with these classes in the Open Images dataset [22]. Let $\mathcal{C}$ denote the set of all detectable classes by either of these two detectors. For a frame F_r, the FRCNN model produces a set of M quadruples: $\left\{\left(C_r^i, B_r^i, F_r^i, S_r^i\right)\right\}_{i=1}^{M} = \text{FRCNN}(F_r)$, one for each detected object, consisting of the label $C \in \mathcal{C}$ of the detected object, its bounding box B in the frame, a feature vector F characterizing the visual appearance of the object, and a detection confidence S.

Tracking a Sound Source. In order to robustly track the visual trail of a potential sound source between a reference frame F_r and a target frame F_f, we employ RAFT [41] – an off-the-shelf state-of-the-art robust optical flow method. RAFT yields a dense optical flow field for each pixel in the reference frame. We filter this flow field using the bounding boxes B_r^i, and associate it with

the i-th detected sounding object. Next, we base the flow field in a 3D coordinate space using the estimated pseudo-depth map associated with the respective frames; thus allowing for the recovery of the motion track of the sounding object in a 3D space.

Computing the Ground-Truth Displacement Vector. Our proposed flow-based tracking method yields a bounding box of different displacement vectors (one for each pixel in the box) corresponding to every potential sound source in the reference frame F_r. However, as alluded to above, we envisage representing a scene succinctly using a scene graph with each node capturing a single motion vector. To this end, we summarize the flow field associated with a detection box using their the median; thus charaterizing the displacement $\mathbf{d}_i$ of that object in that window.

3.3 Constructing Pseudo-3D Visual Scene Graph

With the object detections in place as described above, we now proceed to construct the *Pseudo-3D Visual Scene Graph* for V. While, for most of the prior approaches [17, 12], all detected objects are trivially added to the graph as nodes, our use-case of sound source separation dictates that the constructed graph permits the learning of correlations between appropriate subgraphs and the separated audio sources. Towards this end, each sound source in a dataset is associated with a set of objects in the visual domain (i.e., from the set of classes $\mathcal{C}$ of FRCNN) which we call *Auditory Objects* and which could potentially create sound. For instance, a *crying* sound could arise from classes such as *kid*, *baby*, etc. Let us denote an auditory object by p, where $p \in \mathcal{C}$. The entire video V could then be thought of as a collection of auditory objects, $P = \{p_1, \ldots, p_N\}$, which together combine to generate the mixed audio $m(t)$. For each of these auditory objects p_i, we identify the subset $\mathcal{V}_{p_i}$ of $M - N$ objects that are non-auditory and overlap with p_i with an Intersection Over Union (IoU) greater than a pre-defined threshold γ. These objects are called *Context Objects*. The vertex set $\mathcal{V}$ of the graph $\mathcal{G}$ associated with video V is then constructed as $\mathcal{V} = \bigcup_{i=1}^{N}(p_i \bigcup \mathcal{V}_{p_i})$.

Next, we describe the process of constructing the edge set $\mathcal{E}$ of the graph $\mathcal{G}$. While prior approaches typically either design dense fully-connected scene-graphs with equal edge weights [7] or deploy a visual relationship detector [12], nonetheless they do not usually embody any 3D scene geometry. Instead in ASMP, we propose to mitigate this shortcoming by constructing the edge weights from the pseudo-3D scene we constructed above. To this end, we first extract 3D point clouds for every object i in frame F_r by leveraging the rectified pseudo-depth map. Let Q_i (for $i = 1, 2, \ldots M$) denote the pseudo 3D point cloud of all pixels associated with node n_i within its corresponding FRCNN bounding box. Note that each point $\mathbf{x}_r^{Q_i} \in Q_i$ is a 3D vector with pixel-normalized $\mathbf{xy}$ coordinates and their pseudo-depths. To define the spatial proximity between two nodes n_i and n_j, we compute the symmetrized Chamfer distance (D_{ij}) [4] between every pair of points in $\mathbf{x}_r^{Q_i}$ and $\mathbf{x}_r^{Q_j}$. These distances are then normalized to be within $[0, 1]$ and used to create a weighted-adjacency matrix defining the graph edges $\mathcal{E}$ by using a radial basis function on the Chamfer distance matrix, i.e., the weight of an edge $e_{ij} = \exp(\frac{-D_{ij}}{\sigma^2})$, for a suitable scale σ, set in our experiments as the median of the entries in the distance matrix.

Visual Encoding of Sounding Interactions: The scene graph $\mathcal{G}$ is a holistic summary of the visual information of V and is the visual analogue to the mixed audio $m(t)$ accompanying V. For the purposes of our task, we are interested in extracting appropriate subgraphs of $\mathcal{G}$ that are capable of inducing a separation of $m(t)$ into its constituents $\mathbf{a}_i(t)$ for $i = \{1, 2, \ldots, N\}$. This is accomplished by employing a recurrent graph attention to segment the graph $\mathcal{G}$ into sub-graphs. To segment the graph $\mathcal{G}$, we first employ a multi-headed graph attention network [45] which operates on the features associated with the scene graph nodes and performs multi-head graph message passing. This allows ASMP to incorporate the spatial scene geometry (from edge weights) and scene context from the neighbors of an auditory node for characterizing the visual representation of a sound source. For capturing the visual representation of interactions (between objects) that produce a sound, we design an edge convolution network [47], the features from which are then simultaneously pooled with the graph attention features using global max-pooling and global average pooling [24] and concatenated. This results in an embedding vector $\boldsymbol{\zeta}$ for the entire graph. Since we need to extract separate sub-graph embeddings to induce a separation of the sound mixture into N sources, we employ a gated recurrent unit (GRU), to recursively extract visual feature vectors $Y = \{\boldsymbol{y}_1, \boldsymbol{y}_2, \ldots, \boldsymbol{y}_N\}$ from $\boldsymbol{\zeta}$. We noticed that extracting a separate background sound from every mixture helps. Thus, our GRU is executed for $N + 1$ steps, rather than N.

To ensure that the extracted graph embeddings Y from the GRU do not repeat a sub-graph, we enforce mutual orthogonality [7] between these embeddings. That is, each embedding $\boldsymbol{y}_i$ emerging out of a recurrence of the GRU is expected to produce a unit-normalized embedding $\hat{\boldsymbol{y}}_i$ that is orthogonal to each of the unit-normalized embeddings generated prior to it, i.e., $\{\hat{\boldsymbol{y}}_1, \hat{\boldsymbol{y}}_2, \ldots, \hat{\boldsymbol{y}}_{i-1}\}$. This constraint is incorporated as a regularization in our training setup. Mathematically, a softer-version of this constraint given by the following is implemented:

$$\mathcal{L}_{\text{ortho}}(Y) = \sum_{i,j \in \{1,2,\ldots,N\}, i \neq j} (\hat{\boldsymbol{y}}_i^\top \hat{\boldsymbol{y}}_j)^2. \tag{1}$$

Acoustic Separator Network: Finally, to induce the separation in the acoustic signal, we incorporate an *Acoustic Separator Network* (ASN), which is a U-Net [37] style encoder-decoder network. Such networks have recently shown promise in sound source separation tasks [16, 27], particularly those that are employed in conditioned settings [11, 29, 52, 39]. The network has three main parts: (i) an *encoder* consisting of a stack of 2D-convolution layers, each coupled with Batch Normalization and Leaky ReLU, (ii) a *bottleneck* layer which concatenates the encoder embedding with the conditioning information, and (iii) a *decoder* which is made up of a series of up-convolution layers, followed by non-linear activations, each coupled with a skip connection from a corresponding layer in the U-Net encoder, matching in spatial resolution of its output. The encoder encodes the input which is a magnitude spectrogram $\mathbf{X} \in \mathbb{R}^{\Omega \times T}$ of a mixed audio $m(t)$, produced via the short-time Fourier transform (STFT), where Ω and T denote the number of frequency bins and the number of video frames, respectively. This encoding is then concatenated with each of the normalized visual encoding vectors $\hat{\boldsymbol{y}}_i$ and decoded to generate a time-frequency mask, $\hat{\mathbf{M}}_i \in [0,1]^{\Omega \times T}$, which when multiplied with the magnitude spectrogram $\mathbf{X}$ of the mixture yields an estimate of the magnitude spectrogram of the separated source $\hat{\mathbf{S}}_i = \hat{\mathbf{M}}_i \odot \mathbf{X}$, where $\odot$ denotes element-wise product. The separated signal in time domain, $\hat{\mathbf{a}}_i(t)$, is then recoverable by applying inverse Short time Fourier Transform (iSTFT).

Direction Prediction Network: Since audio typically only provides a coarse sense of the direction of source motion (say, coming closer or moving farther, etc.), we cast the task of predicting the motion vector $\mathbf{d}_i$ of the auditory object as a classification task. The goal is to predict the octant of a cube into which $\mathbf{d}_i \in \mathbb{R}^3$ belongs, where the center of the cube refers to the 3D centroid of the corresponding graph node. We realize this objective in ASMP by incorporating a classifier network, $\boldsymbol{h}_\Lambda(\cdot)$ with parameters Λ that takes as input the (spectrogram) output of the acoustic separator network.

Note that we compute a separate displacement vector $\mathbf{d}_i$ per window w, while the separated $\hat{\mathbf{S}}_i$ spans the whole length of the video. We thus compute a set of displacement vectors $\{\mathbf{d}_i^w\}_{w=1}^W$, for each window w. Our network takes as input the separated spectrogram, $\hat{\mathbf{S}}_i$, and the visual encoding of the source i ($\hat{\boldsymbol{y}}_i$) and produces as output an estimate of the octant, $\hat{\mathbf{d}}_i^w \in \{0, 1, 2, \ldots, 8\}$, depending on the direction in which the vector lies, where the label 0 signifies no motion. In order to predict the vector for a particular window, appropriate time-aligned slices of $\hat{\mathbf{S}}_i$ are chosen. The sliced spectrogram is then embedded through a ResNet [14] style network. For architectural details of different components of the network, please refer to the supplementary. Thus, we have $\boldsymbol{h}_\Lambda : \hat{\mathbf{S}}_i \rightarrow \{\mathbf{d}_i^w\}_{w=1}^W$.

3.4 Learning Losses

ASMP trains purely with weak/self-supervisory cues. In particular, we train our model by employing the 'mix-and-separate" strategy [11, 9, 51, 52, 7], where the audio tracks from multiple videos (typically 2) are combined with the goal being to separate out the audio for each possible source from the mixture ($\mathbf{X}$). Towards this end, we employ the following set of losses:

Consistency Loss ensures that the separated spectrograms of a particular class of sound source (such as a sound from a guitar, the cry of a baby, etc.) always retains its identity irrespective of which video it comes from [11]. Typically a cross-entropy loss satisfies this requirement. However in ASMP, since the separation is induced by a holistic scene graph recurrently embedded by a GRU, it is not known in advance, in what order the sources are separated. Thus, we consider all possible combinations of the ground truth labels and assign the one with the minimum loss. This is given by:

$$\mathcal{L}_{\text{cons}} = -\sum_{u=1,2} \min_{\sigma^u \in \mathcal{S}_{N_u+1}} \sum_{i=1}^{N_u+1} \sum_{c=1}^{\mathbb{A}} \mathbb{1}_{i,\sigma^u(c)}^u \log p_{i,c}^u, \tag{2}$$

Table 1: SDR, SIR, and SAR results on the ASIW and AVE test sets. [Key: **Best**, second-best results.]

Only Separation	**ASIW**				**AVE**			
	SDR ↑	SIR ↑	SAR ↑	Dir. Acc. (%)↑	SDR ↑	SIR ↑	SAR ↑	Dir. Acc. (%)↑
Sound of Motion (SofM) [51]	6.7	9.4	11.1	-	4.1	9.2	7.6	-
Cyclic Co-Learn [42]	7.0	14.4	12.4	-	4.2	9.7	8.4	-
Co-Separation [11]	6.6	12.9	12.6	-	3.9	9.3	7.8	-
AVSGS [7]	8.8	14.1	13.0	-	5.8	10.4	8.2	-
ASMP (Ours)	**9.4**	**14.7**	**13.7**	-	**6.5**	**12.4**	**8.9**	-
Separation & Dir Pred.	SDR ↑	SIR ↑	SAR ↑	Dir. Acc. (%)↑	SDR ↑	SIR ↑	SAR ↑	Dir. Acc. (%)↑
Majority Vote	-	-	-	35.1	-	-	-	26.5
Sound of Motion (SofM) [51]	7.6	11.7	13.1	38.6	6.2	11.4	9.1	32.2
Cyclic Co-Learn [42]	8.3	14.9	13.2	44.8	6.0	11.1	9.3	31.8
Co-Separation [11]	7.8	13.5	13.3	42.9	5.7	10.4	8.1	28.3
AVSGS [7]	9.1	14.9	13.6	52.7	7.0	12.2	9.5	**34.6**
ASMP (Ours)	**9.9**	**15.3**	**14.1**	**54.6**	**7.6**	**13.6**	**9.9**	34.3

Table 2: SDR, SIR, and SAR Ablation results on the ASIW test set. [Best results in **bold**.]

		ASIW		
Row	Method	SDR [dB]↑	SIR [dB]↑	SAR [dB]↑
1	ASMP (Full Model)	**9.9**	**15.3**	**14.1**
2	ASMP- Multiscale Chamfer	9.6	15.1	14.0
3	ASMP- Only Direction Prediction ($\lambda_1 = \lambda_2 = \lambda_3 = 0$)	6.4	11.2	11.7

where $N_u + 1$ is the number of auditory objects in the u-th video, $\mathcal{S}_{N_u+1}$ indicates the set of all permutations on $\{1, \ldots, N_u + 1\}$, $p^u_{i,c}$ denotes the predicted probability produced by the classifier for class c given $\hat{\mathbf{S}}^u_i$ as input, $\mathbb{1}^u_{i,\sigma^u(c)}$ is an indicator for the ground-truth class of the c-th object in video u, and $\mathbb{A}$ denotes the number of sounding object classes in the dataset.

Cyclic Loss attempts to preserve the cycle consistency of the generated masks of a video. Here the separated masks, corresponding to each of the sources in the video, when added together should yield a mask which separates the audio spectrogram for the whole video from the mixture audios, across two videos. This is given by: $\mathcal{L}_{\text{co-sep}} = \sum_{u=1,2} \left\| \sum_{i=1}^{N_u+1} \hat{\mathbf{M}}^u_i - \mathbf{M}^{\mathbf{u}}_{\text{ibm}} \right\|_{\mathbf{1}}$, where $\mathbf{M}^{\mathbf{u}}_{\text{ibm}} = \mathbb{1}_{\mathbf{X^u} > \mathbf{X^{\neg u}}}$ denotes the binary mask for the audio of video u within the mixture $\mathbf{X}$.

Direction Prediction Loss is a standard cross-entropy loss, which checks for the accuracy of the predicted octant number $\{0, 1, \ldots, 8\}$ for every separated sound source, per window. It is given by:

$$\mathcal{L}_{\text{dirpred}} = -\sum_{u=1,2} \min_{\sigma^u \in \mathcal{S}_{N_u+1}} \sum_{i=1}^{N_u+1} \sum_{w=1}^{W} \sum_{c=0}^{8} \mathbb{1}^{u,w}_{i,\sigma^u(c)} \log q^{u,w}_{i,c}, \tag{3}$$

where $N_u + 1$ is the number of auditory objects in the uth video. $\mathcal{S}_{N_u+1}$ indicates the set of all permutations on $\{1, \ldots, N_u + 1\}$, $q^{u,w}_{i,c}$ denotes the predicted probability produced by the classifier for class c given $\hat{\mathbf{S}}^{u,w}_i$ as input, and $\mathbb{1}^{u,w}_{i,\sigma^u(c)}$ is an indicator of the ground-truth class of the c-th object in video u for window w.

Final Loss of ASMP is given by the following, with weights $\lambda_1, \lambda_2, \lambda_3, \lambda_4 \geq 0$:

$$\mathcal{L} = \lambda_1 \mathcal{L}_{\text{cons}} + \lambda_2 \mathcal{L}_{\text{co-sep}} + \lambda_3 \mathcal{L}_{\text{ortho}} + \lambda_4 \mathcal{L}_{\text{dirpred}}. \tag{4}$$

4 Experiments

4.1 Datasets and Experimental Setup

Audio Separation in the Wild (ASIW) Dataset: Several prior approaches to visually-guided audio source separation present experiments mainly for separating sounds of musical instruments [9, 42]. Such results may not necessarily carry over easily to more generic and natural day to day life contexts. To this end, we consider the recently proposed *Audio Separation in the Wild* (ASIW) dataset [7] for our experiments. This dataset consists of 147 validation, 322 test, and 10,540 training videos crawled from the larger AudioCaps dataset [20]. It has 14 auditory classes, such as *baby cries*, *bell ring*, *birds chirp*, *camera clicks*, *train sounds*, *automobile sounds*, etc. Each video in the dataset is 10s long,

has significant camera motion, and captures diverse audio-visual contexts. To evaluate ASMP for direction prediction, we divide each video into temporal windows of 1s long and predict a discretized 3D direction vector for each window.

Audio Visual Event (AVE) Dataset: Apart from the challenging ASIW dataset, we conduct additional experiments by adapting the popular *Audio Visual Event* (AVE) Dataset [43] for our task. Since this dataset was originally designed for the task of identifying audio-visual events, adapting it for to evaluate our approach is straightforward. We treat each audio-visual event class as an auditory class and associate with it a set of *Auditory Objects* (as discussed before). The dataset contains 2211 training, 257 validation, and 261 test set videos across 29 audio-visual event classes, including potentially-moving object classes such, such as bus, train, dog, horse, banjo, etc. The videos in this dataset are 10s long as well. Similar to ASIW, we divide each video into windows of 1s long for computing the motion displacement vectors.

Baselines: To the best of our knowledge, the task of jointly separating audio sources (using video) and predicting motion directions is a novel task, and thus does not have a prior baseline to compare to. Thus, we compare ASMP against the state-of-the-art methods for audio-visual source separation, specifically those methods that use the "mix-and-separate" learning and also evaluate against them for assessing the efficacy of direction prediction:
Co-Separation [11] uses a single auditory object for conditioning a source separation network.
Sound of Motion (SofM) [51] incorporates object/human appearances and their pixel-level motion trajectories to condition an audio separation network.
Cyclic Co-Learning [42] is a recent method that trains a deep model for the joint task of audio separation and visual grounding of the audio source.
Audio-Visual Scene Graph Segmenter (AVSGS) [7], uses a scene graph for conditioning an audio separator network using the 2D visual context of the audio source.

Evaluation Metrics: We quantify the audio source separation performances using the standard evaluation metrics [52, 11, 42], namely: (i) *Signal-to-Distortion Ratio (SDR)* [in dB] [46, 34] – a higher SDR indicating a more faithful reproduction of the original signal, (ii) *Signal-to-Interference Ratio (SIR)* [in dB] – quantifying the extent of reduction in interference in the estimated signal, and (iii) *Signal-to-Artifact Ratio (SAR)* [in dB] – capturing the extent to which artifacts are introduced by the separator. Further, as our motion direction prediction sub-task is cast as a classification problem in our setup, we also report its classification accuracy (Dir. Acc. ($\%$)).

Implementation Details: For every video in our setup, we detect upto two auditory objects, one background auditory object, and 20 context nodes. The visual feature of the background object is derived from a FRCNN embedding of a random crop of the reference frame F_r. The audio streams are sub-sampled at 11kHz and STFT spectrograms are extracted using a Hann window of size 1022, with hop length of 256, following prior works [11, 52]. We set $\Omega = 256$ and $T = 256$. The embeddings, $\hat{\boldsymbol{y}}_i$, and the GRU-hidden state are 512-dimensional. The IoU threshold, δ is set to 0.1 for both datasets.The weights on the different losses are as follows: $\lambda_1 = 0.05, \lambda_2 = 1.0, \lambda_3 = 1.0, \lambda_4 = 0.05$. Our model is trained using the ADAM optimizer [21] with a weight decay of 1e-4, $\beta_1 = 0.9$, $\beta_2 = 0.999$. The learning rate is set to $1e-4$ and is decreased by a factor of 0.1 every 15K iterations.

4.2 Experimental Results

In Table 1, we present results for the separation and direction prediction model performances of our method versus competing approaches on the ASIW and AVE datasets under two settings: (i) when the models are only trained for separation, (ii) when they are also trained to predict the 3D motions of the sounding objects. Our results clearly attest to the benefit of using the 3D structure of the scene and the motion direction prediction for audio separation. Specifically, ASMP shows a boost of anywhere between 0.3 dB to 1.1 dB on the SDR scale, across the two datasets, when trained to predict the motion direction. Furthermore, the results evince that ASMP out-competes prior approaches in almost all of the evaluation categories, by upto 2.4 db on the SIR scale, for the AVE dataset over the next best (and closely-related) approach of AVSGS [7]. These results clearly demonstrate the generalizability of our method to varied datasets, scene contexts, and audio diversity. From amongst the competing techniques, we find that AVSGS comes closest to matching our performance across the two datasets, which is perhaps unsurprising given that they use a (2D) scene graph to encode the visual context of the sounding object. However, our results show that the presence of 3D scene geometry is also essential for good audio separation.

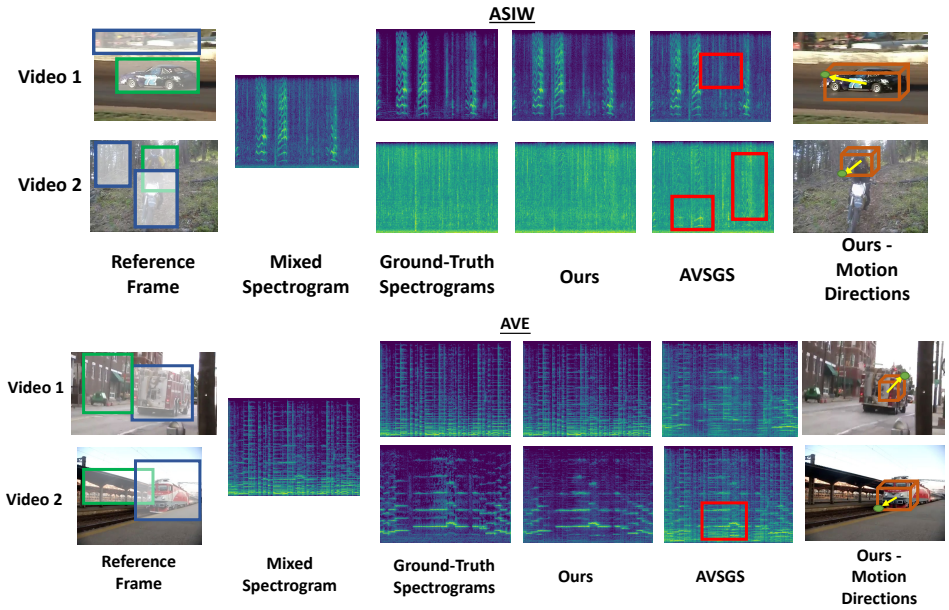

Figure 3: Audio source separation and motion prediction results on ASIW (top) and AVE (bottom). **Bounding boxes** on reference frames show regions attended by ASMP. Red boxes indicate regions of high differences between ground truth and predicted spectrograms. The yellow unit cube shown in the *Motion Directions* images, indicates the object whose motion is predicted. The green dot shows the ground truth motion direction, while the yellow arrow shows the predicted direction by ASMP.

In Table 1, we also report the accuracy of motion prediction of the sounding object (in %) for both ASMP and other baselines. As is clear from the table, we find that the accuracy of direction prediction using ASMP is much better than prior methods (by upto $\sim 2\%$). The gains over a simple majority label prediction is especially pronounced, attesting to the complementary benefits of improved sound source separation and motion estimation. However, there remains room for improvement.

Ablation Study: We report performances of a few key ablated variants of our model in Table 2, on the ASIW dataset, viz. : (i) by computing the weights of the graph edges via a multiscale RBF kernel, (ii) using only the motion direction prediction as a training signal. For the former, we threshold the Chamer distances at multiple (two) scales, viz : (a) the median of the weights and (b) 100th percentile of the weights. This creates a forest of graphs which combined together feed the visual information of the scene into the audio separator network. Our results in Table 2 shows that this approach of graph construction almost levels up to our RBF formulation but falls a bit short, perhaps because of the hard thresholding of edges that occur in this formulation. The other ablated variant of our model which we experiment with, is that of training only with the motion direction prediction loss. As the results bear out, this model variant shows promise but underperforms our full model considerably, corroborating the utility of the other loss terms.

Qualitative Results: In Figure 3, we present sample separation results from the ASIW and AVE test sets, and juxtapose results obtained by our method against the competitive AVSGS baseline. The superiority of our model's separability becomes evident at first glance at the separated spectrograms which mimic the ground truth spectrograms more closely compared to AVSGS. The estimates of the motion directions seems to agree with the ground truth as well. **For further details about the model architecture, more qualitative results, and user studies, please refer to the supplementary.**

5 Conclusions

In this work, we presented ASMP, a novel algorithm to leverage visual scene geometry to induce better separation of a mixed audio signal into its constituents. Towards this end, we incorporate pseudo-3D cues into our algorithmic pipeline via a scene graph data structure. Additionally, our work showcases the effectiveness of introducing additional supervision by predicting the direction of motion of the sound source from the separated audio, which allows our model to further improve on source separation, mitigating the challenges posed by a lack of supervised training data. We exhibit state-of-the-art performances on two challenging "in-the-wild" datasets and plan to make our PyTorch implementation public, upon acceptance.

References

[1] Triantafyllos Afouras, Andrew Owens, Joon Son Chung, and Andrew Zisserman. Self-supervised learning of audio-visual objects from video. In *Proc. ECCV*, 2020.

[2] Sameer Agarwal, Yasutaka Furukawa, Noah Snavely, Ian Simon, Brian Curless, Steven M Seitz, and Richard Szeliski. Building rome in a day. *Communications of the ACM*, 54(10):105–112, 2011.

[3] Relja Arandjelovic and Andrew Zisserman. Objects that sound. In *Proc. ECCV*, pages 435–451, 2018.

[4] Harry G Barrow, Jay M Tenenbaum, Robert C Bolles, and Helen C Wolf. Parametric correspondence and chamfer matching: Two new techniques for image matching. Technical report, SRI INTERNATIONAL MENLO PARK CA ARTIFICIAL INTELLIGENCE CENTER, 1977.

[5] Paul J Besl and Neil D McKay. Method for registration of 3-d shapes. In *Sensor fusion IV: control paradigms and data structures*, volume 1611, pages 586–606. Spie, 1992.

[6] Moitreya Chatterjee and Anoop Cherian. Sound2sight: Generating visual dynamics from sound and context. In *Proc. ECCV*. Springer, 2020.

[7] Moitreya Chatterjee, Jonathan Le Roux, Narendra Ahuja, and Anoop Cherian. Visual scene graphs for audio source separation. In *Proc. ICCV*, 2021.

[8] Ariel Ephrat, Inbar Mosseri, Oran Lang, Tali Dekel, Kevin Wilson, Avinatan Hassidim, William T Freeman, and Michael Rubinstein. Looking to listen at the cocktail party: a speaker-independent audio-visual model for speech separation. *ACM Trans. Graph. (TOG)*, 37(4):1–11, 2018.

[9] Chuang Gan, Deng Huang, Hang Zhao, Joshua B Tenenbaum, and Antonio Torralba. Music gesture for visual sound separation. In *Proc. CVPR*, pages 10478–10487, 2020.

[10] Ruohan Gao and Kristen Grauman. 2.5 d visual sound. In *Proc. CVPR*, pages 324–333, 2019.

[11] Ruohan Gao and Kristen Grauman. Co-separating sounds of visual objects. In *Proc. ICCV*, pages 3879–3888, 2019.

[12] Shijie Geng, Peng Gao, Chiori Hori, Jonathan Le Roux, and Anoop Cherian. Spatio-temporal scene graphs for video dialog. In *Proc. AAAI*, 2021.

[13] Richard Hartley and Andrew Zisserman. *Multiple view geometry in computer vision*. Cambridge university press, 2003.

[14] Kaiming He, Xiangyu Zhang, Shaoqing Ren, and Jian Sun. Deep residual learning for image recognition. In *Proc. CVPR*, pages 770–778, 2016.

[15] John Hershey and Javier Movellan. Audio vision: Using audio-visual synchrony to locate sounds. In *Proc. NIPS*, pages 813–819, December 1999.

[16] Andreas Jansson, Eric Humphrey, Nicola Montecchio, Rachel Bittner, Aparna Kumar, and Tillman Weyde. Singing voice separation with deep U-net convolutional networks. In *Proc. ISMIR*, October 2017.

[17] Jingwei Ji, Ranjay Krishna, Li Fei-Fei, and Juan Carlos Niebles. Action genome: Actions as compositions of spatio-temporal scene graphs. In *Proc. CVPR*, pages 10236–10247, 2020.

[18] Justin Johnson, Ranjay Krishna, Michael Stark, Li-Jia Li, David Shamma, Michael Bernstein, and Li Fei-Fei. Image retrieval using scene graphs. In *Proc. CVPR*, pages 3668–3678, 2015.

[19] Einat Kidron, Yoav Y Schechner, and Michael Elad. Pixels that sound. In *Proc. CVPR*, volume 1, pages 88–95. IEEE, 2005.

[20] Chris Dongjoo Kim, Byeongchang Kim, Hyunmin Lee, and Gunhee Kim. Audiocaps: Generating captions for audios in the wild. In *Proc. NAACL HLT*, pages 119–132, 2019.

[21] Diederik P Kingma and Jimmy Ba. Adam: A method for stochastic optimization. In *Proc. ICLR*, 2014.

[22] Ivan Krasin, Tom Duerig, Neil Alldrin, Vittorio Ferrari, Sami Abu-El-Haija, Alina Kuznetsova, Hassan Rom, Jasper Uijlings, Stefan Popov, Andreas Veit, et al. Openimages: A public dataset for large-scale multi-label and multi-class image classification. *Dataset available from https://github. com/openimages*, 2(3):18, 2017.

[23] Ranjay Krishna, Yuke Zhu, Oliver Groth, Justin Johnson, Kenji Hata, Joshua Kravitz, Stephanie Chen, Yannis Kalantidis, Li-Jia Li, David A Shamma, et al. Visual Genome: Connecting language and vision using crowdsourced dense image annotations. *Int. J. Comput. Vis.*, 123(1):32–73, 2017.

[24] Junhyun Lee, Inyeop Lee, and Jaewoo Kang. Self-attention graph pooling. In *Proc. ICML*, pages 3734–3743, June 2019.

[25] Sijia Li, Shiguang Liu, and Dinesh Manocha. Binaural audio generation via multi-task learning. *ACM Transactions on Graphics (TOG)*, 40(6):1–13, 2021.

[26] Xiaowei Li, Changchang Wu, Christopher Zach, Svetlana Lazebnik, and Jan-Michael Frahm. Modeling and recognition of landmark image collections using iconic scene graphs. In *Proc. ECCV*, pages 427–440. Springer, 2008.

[27] Yuzhou Liu and DeLiang Wang. Divide and conquer: A deep CASA approach to talker-independent monaural speaker separation. *IEEE/ACM Trans. Audio, Speech, Lang. Process.*, 27(12):2092–2102, 2019.

[28] Bruce D Lucas, Takeo Kanade, et al. An iterative image registration technique with an application to stereo vision. Vancouver, 1981.

[29] Gabriel Meseguer-Brocal and Geoffroy Peeters. Conditioned-U-Net: Introducing a control mechanism in the U-Net for multiple source separations. *arXiv preprint arXiv:1907.01277*, 2019.

[30] Daniel Michelsanti, Zheng-Hua Tan, Shi-Xiong Zhang, Yong Xu, Meng Yu, Dong Yu, and Jesper Jensen. An overview of deep-learning-based audio-visual speech enhancement and separation. *arXiv preprint arXiv:2008.09586*, 2020.

[31] Pedro Morgado, Nuno Vasconcelos, Timothy Langlois, and Oliver Wang. Self-supervised generation of spatial audio for 360° video. In *Proc. NeurIPS*, pages 360–370, 2018.

[32] Andrew Owens and Alexei A Efros. Audio-visual scene analysis with self-supervised multisensory features. In *Proc. ECCV*, pages 631–648, 2018.

[33] Andrew Owens, Phillip Isola, Josh McDermott, Antonio Torralba, Edward H Adelson, and William T Freeman. Visually indicated sounds. In *Proc. CVPR*, pages 2405–2413, 2016.

[34] Colin Raffel, Brian McFee, Eric J Humphrey, Justin Salamon, Oriol Nieto, Dawen Liang, Daniel PW Ellis, and C Colin Raffel. mir_eval: A transparent implementation of common mir metrics. In *Proc. ISMIR*, 2014.

[35] René Ranftl, Alexey Bochkovskiy, and Vladlen Koltun. Vision transformers for dense prediction. In *Proc. ICCV*, 2021.

[36] Shaoqing Ren, Kaiming He, Ross Girshick, and Jian Sun. Faster r-cnn: towards real-time object detection with region proposal networks. *IEEE Trans. Pattern Anal. Mach. Intell.*, 39(6):1137–1149, 2016.

[37] Olaf Ronneberger, Philipp Fischer, and Thomas Brox. U-net: Convolutional networks for biomedical image segmentation. In *Proc. MICCAI*, pages 234–241. Springer, 2015.

[38] Arda Senocak, Tae-Hyun Oh, Junsik Kim, Ming-Hsuan Yang, and In So Kweon. Learning to localize sound source in visual scenes. In *Proc. CVPR*, pages 4358–4366, 2018.

[39] Olga Slizovskaia, Leo Kim, Gloria Haro, and Emilia Gomez. End-to-end sound source separation conditioned on instrument labels. In *Proc. ICASSP*, pages 306–310, May 2019.

[40] Aswin Shanmugam Subramanian, Chao Weng, Shinji Watanabe, Meng Yu, Yong Xu, Shi-Xiong Zhang, and Dong Yu. Directional asr: A new paradigm for e2e multi-speaker speech recognition with source localization. In *Proc. ICASSP*, pages 8433–8437. IEEE, 2021.

[41] Zachary Teed and Jia Deng. Raft: Recurrent all-pairs field transforms for optical flow. In *Proc. ECCV*, pages 402–419. Springer, 2020.

[42] Yapeng Tian, Di Hu, and Chenliang Xu. Cyclic co-learning of sounding object visual grounding and sound separation. In *Proc. CVPR*, 2021.

[43] Yapeng Tian, Jing Shi, Bochen Li, Zhiyao Duan, and Chenliang Xu. Audio-visual event localization in unconstrained videos. In *Proc. ECCV*, pages 247–263, 2018.

[44] Efthymios Tzinis, Scott Wisdom, Aren Jansen, Shawn Hershey, Tal Remez, Daniel PW Ellis, and John R Hershey. Into the wild with AudioScope: Unsupervised audio-visual separation of on-screen sounds. In *Proc. ICLR*, 2021.

[45] Petar Veličković, Guillem Cucurull, Arantxa Casanova, Adriana Romero, Pietro Lio, and Yoshua Bengio. Graph attention networks. In *Proc. ICLR*, April 2018.

[46] Emmanuel Vincent, Rémi Gribonval, and Cédric Févotte. Performance measurement in blind audio source separation. *IEEE Trans. Audio, Speech, Lang. Process.*, 14(4):1462–1469, July 2006.

[47] Yue Wang, Yongbin Sun, Ziwei Liu, Sanjay E Sarma, Michael M Bronstein, and Justin M Solomon. Dynamic graph CNN for learning on point clouds. *ACM Trans. Graph. (TOG)*, 38(5):1–12, 2019.

[48] Wenjie Xu, Maoshen Jia, Shang Gao, and Lu Li. Multiple sound source separation by using doa estimation and ica. In *2021 4th International Conference on Information Communication and Signal Processing (ICICSP)*, pages 249–253. IEEE, 2021.

[49] Xudong Xu, Hang Zhou, Ziwei Liu, Bo Dai, Xiaogang Wang, and Dahua Lin. Visually informed binaural audio generation without binaural audios. In *Proc. CVPR*, 2021.

[50] Chaoqiang Zhao, Qiyu Sun, Chongzhen Zhang, Yang Tang, and Feng Qian. Monocular depth estimation based on deep learning: An overview. *Science China Technological Sciences*, 63(9):1612–1627, 2020.

[51] Hang Zhao, Chuang Gan, Wei-Chiu Ma, and Antonio Torralba. The sound of motions. In *Proc. ICCV*, pages 1735–1744, 2019.

[52] Hang Zhao, Chuang Gan, Andrew Rouditchenko, Carl Vondrick, Josh McDermott, and Antonio Torralba. The sound of pixels. In *Proc. ECCV*, pages 570–586, 2018.

[53] Yipin Zhou, Zhaowen Wang, Chen Fang, Trung Bui, and Tamara L Berg. Visual to sound: Generating natural sound for videos in the wild. In *Proc. CVPR*, pages 3550–3558, 2018.

Checklist

1. For all authors...
   (a) Do the main claims made in the abstract and introduction accurately reflect the paper's contributions and scope? [Yes]
   (b) Did you describe the limitations of your work? [Yes] Primarily in the Experimental Results subsection.
   (c) Did you discuss any potential negative societal impacts of your work? [N/A] Our algorithm targets an already well established task, which has potentially beneficial applications for speech/music separation, etc.
   (d) Have you read the ethics review guidelines and ensured that your paper conforms to them? [Yes]
2. If you are including theoretical results...
   (a) Did you state the full set of assumptions of all theoretical results? [N/A]
   (b) Did you include complete proofs of all theoretical results? [N/A]
3. If you ran experiments...
   (a) Did you include the code, data, and instructions needed to reproduce the main experimental results (either in the supplemental material or as a URL)? [Yes] The datasets we use are all public [7, 43]. And the code is made available with the Supplemental Material.
   (b) Did you specify all the training details (e.g., data splits, hyperparameters, how they were chosen)? [Yes] Details are available in the Implementation Details and the Datasets and Experimental Setup subsection.
   (c) Did you report error bars (e.g., with respect to the random seed after running experiments multiple times)? [No] Primarily because the performance gains obtained were quite significant. All experiments were conducted with the same seed.
   (d) Did you include the total amount of compute and the type of resources used (e.g., type of GPUs, internal cluster, or cloud provider)? [Yes] See the supplementary material.

4. If you are using existing assets (e.g., code, data, models) or curating/releasing new assets...
   (a) If your work uses existing assets, did you cite the creators? [Yes]
   (b) Did you mention the license of the assets? [No]
   (c) Did you include any new assets either in the supplemental material or as a URL? [N/A]
   (d) Did you discuss whether and how consent was obtained from people whose data you're using/curating? [N/A]
   (e) Did you discuss whether the data you are using/curating contains personally identifiable information or offensive content? [N/A]
5. If you used crowdsourcing or conducted research with human subjects...
   (a) Did you include the full text of instructions given to participants and screenshots, if applicable? [N/A]
   (b) Did you describe any potential participant risks, with links to Institutional Review Board (IRB) approvals, if applicable? [N/A]
   (c) Did you include the estimated hourly wage paid to participants and the total amount spent on participant compensation? [N/A]